J. Fluid Mech. (1983), *vol.* 129, *pp.* 137–151
Printed in Great Britain

The contraction of contaminant distributions in reversing flows

By RONALD SMITH

Department of Applied Mathematics and Theoretical Physics, University of Cambridge, Silver Street, Cambridge CB3 9EW

(Received 22 October 1982)

Exact expressions are derived for the centroid and variance as functions across the flow when there has been an initially uniform contaminant release in an oscillatory flow. Two examples are given to demonstrate that there can be a substantial region of the flow (where the velocity shear is relatively large) in which the contaminant distribution exhibits contraction after flow reversal. This effect, and the sensitivity of the variance to the precise time of discharge, is most marked when the flow oscillations are rapid relative to the timescale for cross-sectional mixing.

1. Introduction

For the particular case of an oscillatory unbounded linear shear flow, the author (Smith 1982*b*) has shown that in each longitudinal slice of the contaminant cloud the variance was increasing. Yet, after flow reversal, the relative movement of the slices gave the impression of an overall contraction (Smith 1982*b*, figures 3, 4). The question that motivated the present investigation was whether the contraction after flow reversal in bounded shear flows might likewise only be an artifact of the cross-sectional averaging process.

The answer to the question turns out to be that there is a substantial region (where the velocity shear is relatively large) in which the variance does exhibit contraction after flow reversal. Moreover, if cross-sectional mixing takes place on a longer timescale than the flow oscillations, then the contractions are quite prolonged and of large amplitude.

2. Hermite-series representation

For mathematical simplicity, we shall assume that the excursion distance within one flow oscillation is sufficiently small that the flow can be regarded as being longitudinally uniform (i.e. independent of x). Thus the advection–diffusion equation for the contaminant concentration $c(x, y, z, t)$ takes the form

$$\partial_t c + u\,\partial_x c = \kappa\,\partial_x^2 c + \nabla.(\kappa \nabla c), \tag{2.1a}$$

with

$$\kappa \mathbf{n}.\nabla c = 0 \quad \text{on } \partial A. \tag{2.1b}$$

Here $u(y, z, t)$ is the longitudinal velocity $\kappa(y, z, t)$ the diffusivity, ∇ the transverse gradient operator $(0, \partial_y, \partial_z)$, A the flow region, ∂A its boundary, and $\mathbf{n}$ the outward normal.

Following Smith (1982*c*) we pose the Hermite-series representation for c:

$$c = \frac{M}{(2\pi)^{\frac{1}{2}}\sigma} \exp\left(-\tfrac{1}{2}\xi^2\right) \left\{ a^{(0)} + \sum_{m=3}^{\infty} \frac{a^{(m)}(y, z, t)\,\mathrm{He}_m(\xi)}{\sigma^m} \right\}, \tag{2.2a}$$

with

$$\xi = \frac{x - \int_0^t \bar{u}(t')\,dt' - X}{\sigma}. \tag{2.2b}$$

Here M is the volume discharge per unit area of the flow region, $\bar{u}(t)$ the cross-sectionally averaged velocity $X(y,z,t)$ the centroid displacement relative to a point of reference moving with the bulk velocity, and $\sigma(y,z,t)$ the standard deviation. The Hermite polynomials $\mathrm{He}_m(\xi)$ are defined recursively

$$\mathrm{He}_{m+2} = \xi\,\mathrm{He}_{m+1} - (m+1)\,\mathrm{He}_m, \quad \text{with} \quad \mathrm{He}_0 = 1. \tag{2.3}$$

This Hermite-series approach is very closely related to Aris' (1956) method of moments. However, instead of generating successive moments, the present approach yields successive approximations for the contaminant distribution. For example, if only a_0, X and σ^2 are evaluated, then at each level across the flow we have a Gaussian approximation for c.

The coefficient of $\mathrm{He}_m(\xi)$ in (2.1a) yields the transverse diffusion equation (Smith 1982c, equation (2.7)):

$$\begin{aligned}\partial_t a^{(m)} - \nabla\cdot(\kappa\nabla a^{(m)}) = {} & (u-\bar{u}-\partial_t X)\,a^{(m-1)} + \kappa\nabla X\cdot\nabla a^{(m-1)} \\ & + \nabla\cdot(\kappa\alpha^{(m-1)}\nabla X) + \tfrac{1}{2}\{(2\kappa - \partial_t\sigma^2)\,a^{(m-2)} + \kappa\nabla\sigma^2\cdot\nabla a^{(m-2)} \\ & + \nabla\cdot(\kappa a^{(m-2)}\nabla\sigma^2) - 2\kappa(\nabla X)^2 a^{(m-2)}\} \\ & + \kappa\nabla X\cdot\nabla\sigma^2 a^{(m-3)} + \tfrac{1}{4}\kappa(\nabla\sigma^2)^2\,a^{(m-4)},\end{aligned} \tag{2.4a}$$

with

$$\kappa\mathbf{n}\cdot\nabla a^{(m)} = -a^{(m-1)}\kappa\mathbf{n}\cdot\nabla X - \tfrac{1}{2}a^{(m-2)}\kappa\mathbf{n}\cdot\nabla\sigma^2 \quad \text{on } \partial A. \tag{2.4b}$$

We shall make the simplifying assumption that the discharge is uniform. Thus, the solution for $a^{(0)}$ is

$$a^{(0)} = 1, \tag{2.5}$$

and the starting conditions for (2.4a,b) take the form

$$X = 0, \quad \sigma^2 = \text{constant} \quad \text{at} \quad t = t_0, \tag{2.6}$$

where we have taken the discharge centroid to define the origin $x = 0$.

3. Centroid displacement

To make analytical progress with (2.4a,b), we need the further simplifying assumption that $\kappa(y,z,t)$ remains spatially self-similar (i.e. all positions vary together). For example, in a shallow estuary κ varies with the strength of the tidal current. Thus, for the similarity assumption to be valid it suffices that the current has negligible phase lag across the estuary. Following Smith (1982a) we then introduce the eigenfunctions $\psi_m(y,z)$:

$$\nabla\cdot(\langle\kappa\rangle\nabla\psi_m) + \lambda_m\psi_m = 0, \tag{3.1a}$$

with

$$\langle\kappa\rangle\mathbf{n}\cdot\nabla\psi_m = 0 \quad \text{on } \partial A, \tag{3.1b}$$

where the angle brackets $\langle\ldots\rangle$ denote time averaging. Without loss of generality we assume that the eigenfunctions are normalized such that

$$\psi_0 = 1, \quad \overline{\psi_n^2} = 1. \tag{3.2a,b}$$

At $m = 1$ the absence of $a^{(1)}$ permits us to write (2.4a) as an equation for the centroid displacement:

$$\partial_t X - \nabla . (\kappa \nabla X) = u - \bar{u}, \tag{3.3a}$$

with

$$\kappa \mathbf{n} . \nabla X = 0 \quad \text{on } \partial A. \tag{3.3b}$$

To represent the forcing term we introduce the coefficients

$$u_m(t) = \overline{u\psi_m}, \quad \text{i.e.} \quad u(y,z,t) = \bar{u}(t) + \sum_{m=1}^{\infty} u_m(t)\,\psi_m(y,z). \tag{3.4}$$

This leads to an eigenfunction expansion for X:

$$X = \sum_{m=1}^{\infty} \psi_m(y,z) \int_{t_0}^{t} u_m(t') \exp\left(-\lambda_m T(t',t)\right) dt', \tag{3.5}$$

with

$$T(t',t) = \int_{t'}^{t} \frac{\kappa(t'')}{\langle \kappa \rangle} dt''. \tag{3.6}$$

The integral T can be thought of as being an effective time coordinate for flows with time-dependent turbulent intensities.

For the particular case in which κ is independent of time, and the velocity field is sinusoidal

$$u_m = \alpha_m U \sin(\omega t + \theta_m), \tag{3.7}$$

we can evaluate the integrals (3.5), (3.6) to obtain

$$X = \sum_{m=1}^{\infty} \psi_m(y,z) \frac{\alpha_m U \lambda_m}{\omega^2 + \lambda_m^2} \left\{ \sin(\omega t + \theta_m) - \frac{\omega}{\lambda_m} \cos(\omega t + \theta_m) \right.$$
$$\left. - \exp\left(-\lambda_m (t - t_0)\right) \left[\sin(\omega t_0 + \theta_m) - \frac{\omega}{\lambda_m} \cos(\omega t_0 + \theta_m) \right] \right\}. \tag{3.8}$$

4. Variance

The coefficient $a^{(2)}$ is absent in the representation (2.2a). Thus, at $m = 2$, we have an equation for the horizontal variance σ^2:

$$\partial_t \sigma^2 - \nabla . (\kappa \nabla \sigma^2) = 2\kappa + 2\kappa (\nabla X)^2, \tag{4.1a}$$

with

$$\kappa \mathbf{n} . \nabla \sigma^2 = 0 \quad \text{on } \partial A, \tag{4.1b}$$

$$\sigma^2 = \sigma^2(t_0) \quad \text{at} \quad t = t_0. \tag{4.1c}$$

The positivity of the source terms together with the impermeability of the boundary ensures that σ^2 is positive with an overall tendency to increase with time. However, when $(\nabla X)^2$ drops to zero (after flow reversal) σ^2 can temporarily reduce if there are regions in which $2\kappa + \nabla . (\kappa \nabla \sigma^2)$ is negative.

To obtain an explicit solution for $\sigma^2(y,z,t)$ we make the decomposition (Smith 1982c, equation (4.2))

$$\sigma^2 = \sigma^2(t_0) + K + V - X^2, \tag{4.2}$$

where K and V respectively are associated with the longitudinal diffusion and with the shear:

$$\partial_t K - \nabla . (\kappa \nabla K) = 2\kappa, \tag{4.3a}$$

$$\partial_t V - \nabla . (\kappa \nabla V) = 2X(u - \bar{u}). \tag{4.3b}$$

By analogy with (3.4)–(3.6) we introduce the coefficients

$$\kappa_m(t) = \overline{\kappa \psi_m}, \tag{4.4}$$

and obtain the solution

$$K = 2\int_{t_0}^{t} \bar{\kappa}(t')\,dt' + 2\sum_{m=1}^{\infty} \psi_m(y,z)\int_{t_0}^{t} \kappa_m(t')\exp\left(-\lambda_m\, t(t',t)\right)dt'. \tag{4.5}$$

(For high-Péclet-number flows, where shear dominates diffusion, this contribution to σ^2 can be neglected).

It happens that the constant coefficient $\overline{V}$ in the eigenfunction expansion for $V(y,z,t)$ is precisely the shear-dispersion contribution to the variance for the cross-sectionally averaged concentration (Smith 1982*a*, equation (3.6)),

$$\begin{aligned}\frac{d\overline{V}}{dt} &= 2\overline{(u-\bar{u})X} = 2D(t,t_0)\\ &= 2\sum_{m=1}^{\infty} u_m(t)\int_{t_0}^{t} u_m(t')\exp\left(-\lambda_m\, T(t',t)\right)dt',\end{aligned} \tag{4.6}$$

where $D(t,t_0)$ is the time-dependent shear-dispersion coefficient. It is the time lag between the $u_m(t), u_m(t')$ terms which give rise to the characteristic negative apparent diffusivity following flow reversal (Smith 1982*a*, figures 1*a–c*). Likewise, it is this decorrelation that leads to the marked reduction in the long-term averaged shear dispersion coefficient for rapidly oscillatory flows (Holley, Harleman & Fischer 1970; Chatwin 1975).

For the particular case in which K is independent of time, and the velocity field is sinusoidal, we have (Smith 1982*a*, equation (3.10)):

$$\begin{aligned}\overline{V} = U^2 \sum_{m=1}^{\infty} \frac{\alpha_m^2}{\omega^2+\lambda_m^2}\Big\{&\lambda_m(t-t_0) + \frac{\omega^2-\lambda_m^2}{\omega^2+\lambda_m^2} + \tfrac{1}{2}\cos 2(\omega t+\theta_m)\\ &+\tfrac{1}{2}\cos 2(\omega t_0+\theta_m) - \frac{1}{2}\frac{\lambda_m}{\omega}\sin 2(\omega t+\theta_m) + \frac{1}{2}\frac{\lambda_m}{\omega}\sin 2(\omega t_0+\theta_m)\\ &+ \frac{2\exp\left(-\lambda_m(t-t_0)\right)}{\omega^2+\lambda_m^2}\left[\lambda_m\sin(\omega t+\theta_m)+\omega\cos(\omega t+\theta_m)\right]\\ &\times\left[\lambda_m\sin(\omega t_0+\theta_m)-\omega\cos(\omega t_0+\theta_m)\right]\Big\}.\end{aligned} \tag{4.7}$$

The non-homogeneous term in (4.3*b*) leads us to introduce the further notation

$$u_{mn}(t) = \overline{u\psi_m\psi_n}, \quad u\psi_n = u_n + \sum_{m=1}^{\infty} u_{mn}\psi_m. \tag{4.8a, b}$$

Thus the ψ_m coefficient V_m in the eigenfunction expansion for V satisfies the equation

$$\frac{dV_m}{dt} + \lambda_m\left(\frac{\partial T}{\partial t}\right)V_m = 2\sum_{n=1}^{\infty}\left(u_{mn}(t)-\delta_{mn}\bar{u}\right)\int_{t_0}^{t} u_n(t')\exp\left(-\lambda_n\, T(t',t)\right)dt'. \tag{4.9}$$

If the velocity field is sinusoidal

$$u_{mn}(t)-\delta_{mn}\bar{u}(t) = \alpha_{mn}\,U\sin(\omega t+\theta_{mn}), \tag{4.10}$$

and κ is independent of time, we have

$$\begin{aligned}V_m = \sum_{n=1}^{\infty}\frac{\alpha_{mn}\alpha_n U^2}{\omega^2+\lambda_n^2}\Big\{&\left[\frac{\lambda_n}{\lambda_m}\cos(\theta_{mn}-\theta_n) - \frac{\omega}{\lambda_m}\sin(\theta_{mn}-\theta_n)\right]\left[1-\exp\left(-\lambda_m(t-t_0)\right)\right]\\ &+\frac{2\omega^2-\lambda_m\lambda_n}{4\omega^2+\lambda_m^2}\left[\cos(2\omega t+\theta_{mn}+\theta_n)-\exp\left(-\lambda_m(t-t_0)\right)\cos(2\omega t_0+\theta_{mn}+\theta_n)\right]\end{aligned}$$

$$-\frac{\omega(2\lambda_n+\lambda_m)}{4\omega^2+\lambda_m^2}[\sin(2\omega t+\theta_{mn}+\theta_n)-\exp(-\lambda_m(t-t_0))\sin(2\omega t_0+\theta_{mn}+\theta_n)]$$

$$-\frac{2[\lambda_n\sin(\omega t_0+\theta_n)-\cos(\omega t_0+\theta_n)]}{\omega^2+(\lambda_m-\lambda_n)^2}\{\exp(-\lambda_n(t-t_0))[(\lambda_m-\lambda_n)\sin(\omega t+\theta_m)$$

$$-\omega\cos(\omega t+\theta_{mn})]-\exp(-\lambda_m(t-t_0))[(\lambda_m-\lambda_n)\sin(\omega t_0+\theta_{mn})$$

$$-\omega\cos(\omega t_0+\theta_{mn})]\}. \tag{4.11}$$

The full expression for $V(y,z,t)$ is

$$V=\overline{V}(t)+\sum_{m=1}^{\infty}V_m(t)\,\psi_m(y,z), \tag{4.12}$$

with $\overline{V}$, V_m given by the series (4.7), (4.11).

5. Skewness and spikiness

The increase in complexity from the solution (3.8) for X to the composite series (4.7), (4.11), (4.12) for V deters us from continuing the exact analysis to higher orders. However, the equation for $a^{(3)}$

$$\partial_t a^{(3)}-\nabla.(\kappa\nabla a^{(3)})=\kappa\nabla X.\nabla\sigma^2, \tag{5.1a}$$

with

$$\kappa\mathbf{n}.\nabla a^{(3)}=0 \quad \text{on } \partial A, \tag{5.1b}$$

permits us to make some simple qualitative deductions. For example, in a high-Péclet-number flow at small times after discharge we have the Taylor series

$$a^{(3)}\sim a^{(3)}(t_0)+\tfrac{2}{15}\kappa\nabla u.\nabla\{\kappa(\nabla u)^2\}(t-t_0)^5 \tag{5.2}$$

(Smith 1982*c*, equation (5.2)). Thus for a symmetric discharge, with the initial condition $a^{(3)}(t_0)=0$, the skewness at any individual y,z level develops extremely slowly.

At large times after discharge the expression (3.8) for X only involves the first harmonics $\cos\omega t$, $\sin\omega t$, while the coefficients V_m given by (4.11) involve only the even terms 1, $\cos 2\omega t$, $\sin 2\omega t$. Thus the source term in (5.1*a*) becomes oscillatory (with frequencies $\omega, 3\omega$), and hence $a^{(3)}$ remains bounded. This has the consequence that the skewness $3!\,a^{(3)}/\sigma^3$ eventually decays as $(t-t_0)^{-\frac{3}{2}}$ (Smith 1982*a*, figure 4; Allen 1982, figures 6*b*, 7*b*).

At $m=4$ (2.4*a*, *b*) become

$$\partial_t a^{(4)}-\nabla.(\kappa\nabla a^{(4)})=(u-\bar{u}-\partial_t X)\,a^{(3)}+\kappa\nabla X.\nabla a^{(3)}+\nabla.(\kappa a^{(3)}\nabla X)+\tfrac{1}{4}\kappa(\nabla\sigma^2)^2, \tag{5.3a}$$

with

$$\kappa\mathbf{n}.\nabla a^{(4)}=0 \quad \text{on } \partial A. \tag{5.3b}$$

For high-Péclet-number flows the forcing terms are of order $(t-t_0)^6$, and hence $a^{(4)}$ initially grows as $(t-t_0)^7$. This confirms the usefulness of the Gaussian approximation at small times after discharge. However, at large times there is a constant component in the source terms, as well as the even frequencies $2\omega, 4\omega$. Thus $a^{(4)}$ eventually grows linearly with time and the spikiness (kurtosis) $4!\,a^{(4)}/\sigma^4$ only decays as $(t-t_0)^{-1}$. Consideration of higher-order Hermite coefficients reveals this to be the dominant error contribution in the Gaussian truncation.

Chatwin (1970) shows that for steady flows $a^{(3)}$ and $a^{(4)}$ both eventually grow linearly with time. Thus for steady flows the dominant error is associated with the skewness, and this error decays at the extremely slow rate $(t-t_0)^{-\frac{1}{2}}$. Indeed, the

magnitude of the skewness is such that Smith (1982*c*) concludes that for steady flows the usefulness of the Gaussian approximation is restricted to about one *e*-folding time $1/\lambda_1$ after discharge. For the oscillatory flow case the spikiness (kurtosis) initially grows more slowly and eventually decays more rapidly than does the steady-flow skewness. Hence we can be more optimistic about the accuracy of the Gaussian approximation for contaminant dispersion in oscillatory flows.

6. Vertical shear dispersion in a flow with a parabolic velocity profile

Bowden & Fairbairn (1952) give field observations of the velocity profile in the sea. Their suggested empirical formula is

$$u = 1{\cdot}15U'\left[0{\cdot}63+0{\cdot}37\left(1-\frac{z^2}{h^2}\right)\right]\sin\omega t, \tag{6.1a}$$

where U' is the depth-averaged tidal amplitude and h is the water depth. For algebraic convenience we rewrite this formula:

$$u = U\left[2{\cdot}554+\frac{3}{2}\left(1-\frac{z^2}{h^2}\right)\right]\sin\omega t, \tag{6.1b}$$

with

$$U = 0{\cdot}2837U'. \tag{6.1c}$$

The bulk-flow term $2{\cdot}554U$ does not contribute to the dispersion. Thus we can interpret U as being the effective amplitude of an oscillatory plane Poiseuille flow.

Following Allen (1982), we take the vertical diffusivity κ to be constant (independent of both z and t). Thus the eigenfunctions ψ_m and the velocity coefficients α_m, α_{mn} can be inferred from the steady-flow results (Smith 1982*c*, equation (8.2)):

$$\psi_m = \sqrt{2}\cos\frac{m\pi z}{h}, \quad \lambda_m = \frac{m^2\pi^2\kappa}{h^2}, \tag{6.2a,b}$$

$$\alpha_m = \frac{(-1)^{m+1}3\sqrt{2}}{m^2\pi^2}, \quad \theta_m = \theta_{mm} = \theta_{mn} = 0, \tag{6.2c,d}$$

$$\alpha_{mm} = \frac{3}{4m^2\pi^2}, \quad \alpha_{mn} = (-1)^{m+n+1}\frac{6(m^2+n^2)}{\pi^2(m^2-n^2)^2}. \tag{6.2e,f}$$

(Strictly, a time-independent κ is only appropriate for deep estuaries. Thus the results given below are qualitatively but not quantitatively accurate for intermediate-depth estuaries.)

From (3.8) we find that the centroid displacement is given by the formula

$$X = \frac{6Uh^2}{\pi^4\kappa}\sum_{m=1}^{\infty}\frac{(-1)^m\cos(m\pi z/h)}{m^4+\Omega^2}\left\{\sin\omega t-\frac{\Omega}{m^2}\cos\omega t - \exp\left(-\frac{m^2}{\Omega}\omega(t-t_0)\right)\left[\sin\omega t_0-\frac{\Omega}{m^2}\cos\omega t_0\right]\right\}, \tag{6.3a}$$

with

$$\Omega = \frac{\omega}{\lambda_1} = \frac{\omega h^2}{\pi^2\kappa}. \tag{6.3b}$$

The dimensionless frequency Ω indicates whether the oscillations are sufficiently slow for the dispersion process to be quasi-steady (Bowden 1965), or so fast that the memory of the initial discharge time t_0 persists for several flow oscillations. Figures 1(*a*, *b*, *c*) show that the centroid displacements at the depths $z/h = 0, -\frac{1}{2}, -1$ for the

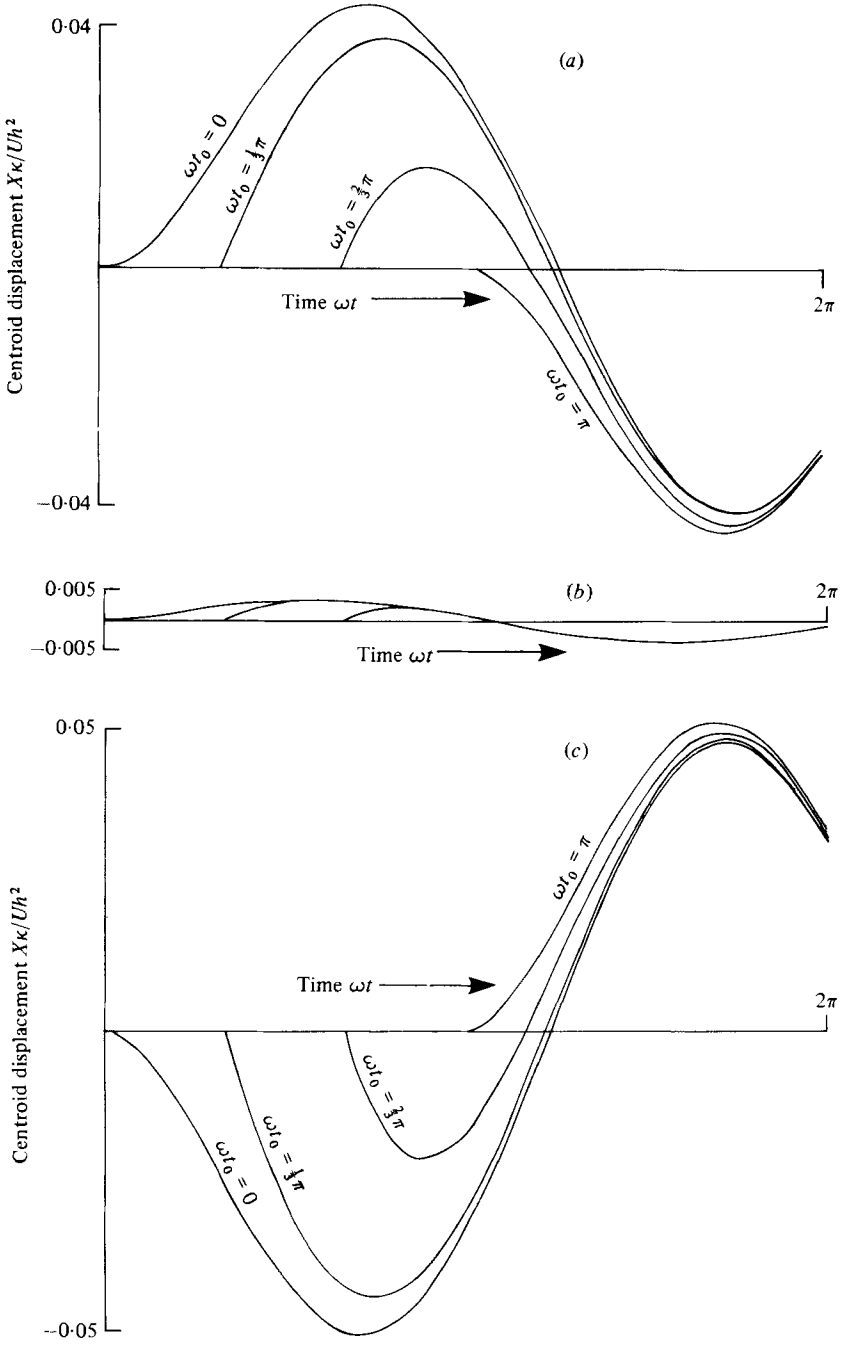

FIGURE 1. Centroid displacements as a function of time at depths (*a*) $z = 0$, (*b*) $z = -\frac{1}{2}h$, (*c*) $z = -h$ in an oscillatory flow with a parabolic velocity profile.

intermediate dimensionless frequency $\Omega = 1$, and with the discharges taking place at the phases $\omega t_0 = 0, \frac{1}{3}\pi, \frac{2}{3}\pi$. At the mid-depth (figure 1*b*) the lowest mode does not contribute to X. Thus not only are the displacements relatively small, but also there is a much more rapid approach to the asymptotic sinusoidal solution than is the case for the other two depths.

If we exclude transient exponential terms, then the solutions (4.7), (4.11) for $\overline{V}$ and V_m take the forms

$$\overline{V} = \frac{18}{\pi^8}\left(\frac{Uh^2}{\kappa}\right)^2 \sum_{m=1}^{\infty} \frac{1}{(m^4+\Omega^2)\,m^4}\left\{\frac{m^2}{\Omega}\omega(t-t_0) + \frac{\Omega^2-m^4}{\Omega^2+m^4} + \tfrac{1}{2}(\cos 2\omega t + \cos 2\omega t_0) - \frac{1}{2}\frac{m^2}{\Omega}(\sin 2\omega t - \sin 2\omega t_0)\right\}, \tag{6.4}$$

$$V_m = \frac{9}{\pi^8 2\sqrt{2}}\left(\frac{Uh^2}{\kappa}\right)^2 \frac{(-1)^{m+1}}{(m^4+\Omega^2)\,m^4}\left\{1 + \frac{2\Omega^2-m^4}{4\Omega^2+m^4}\cos 2\omega t - \frac{4\Omega m^2}{4\Omega^2+m^4}\sin 2\omega t\right\} + \frac{36}{\pi^8\sqrt{2}}\left(\frac{Uh^2}{\kappa}\right)^2 (-1)^m \sum_{n\neq m} \frac{m^2+n^2}{(n^4+\Omega^2)\,(m^2-n^2)^2 n^2} \times\left\{\frac{n^2}{m^2} + \frac{2\Omega^2-n^2m^2}{4\Omega^2+m^4}\cos 2\omega t - \frac{2(m^2+n^2)\,\Omega}{4\Omega^2+m^2}\sin 2\omega t\right\}. \tag{6.5}$$

This asymptotic expression (6.5) for V_m does not involve t_0. Thus the persistent influence of the discharge time t_0 is uniform across the flow. The greatest overall increase in dilution occurs if the contaminant is released at the time

$$\tan 2\omega t_0 = \sum_{m=1}^{\infty} \frac{1}{(m^4+\Omega^2)\,m^2\Omega} \Big/ \sum_{m=1}^{\infty} \frac{1}{(m^4+\Omega^2)\,m^4} \tag{6.6}$$

(i.e. shifting from $\omega t_0 = \frac{1}{4}\pi$ for small Ω to $\omega t_0 = 0$ for large Ω). Figure 2 shows the evolution of $\overline{V}$, including the transient terms, for the case $\Omega = 1$. In keeping with the results of Smith (1982*a*), there is a substantial span of time in which $\overline{V}$ decreases. This would be even more pronounced if a larger value for Ω had been chosen.

The central question towards which the present work is directed is whether the contraction might only be an artifact of the cross-sectional averaging process. For high-Péclet-number flows this can be investigated by plotting the shear-dispersion contribution $V - X^2$ to the variance $\sigma^2(z,t)$. Figures 3(*a*, *b*, *c*) show the results at the depths $z/h = 0, -\frac{1}{2}, -1$ for the case $\Omega = 1$. It is only at the free surface that the contraction is entirely removed. At the other two depths (figures 3*b*, *c*), the time span for contraction is less than in figure 2, but is nevertheless still present. (Away from the free surface the shear-dispersion processes is efficient and the concentration is relatively low. Thus at the turn of the tide there is diffusion downwards and the concentration *increases*.)

7. Comparison with Allen's random-walk results

Although the primary concern of the work of Allen (1982) was with the vertically averaged concentration, her random-walk method also yields the full two-dimensional concentration distribution. She has kindly provided some of her computer output to permit a test of the present Gaussian approximation. A more comprehensive investigation of the numerical accuracy is being undertaken at the University of Oxford by Stairmand (personal communication).

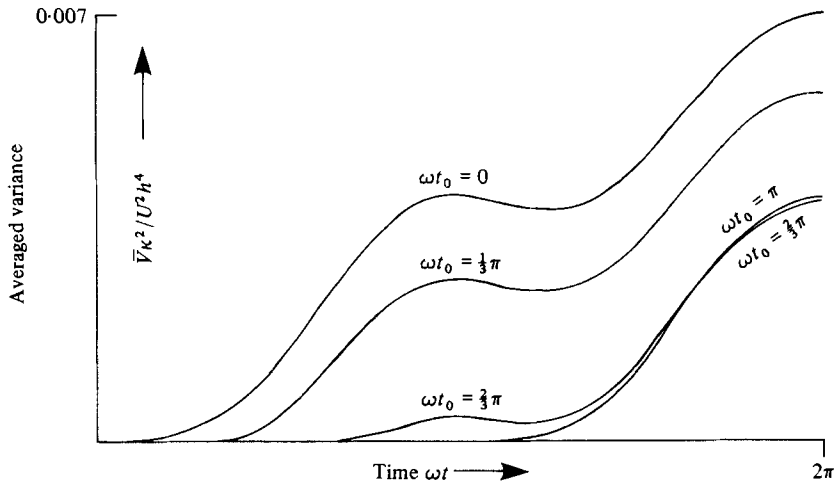

FIGURE 2. The cross-sectionally averaged variance (or the variance of the cross-sectionally averaged concentration) for an oscillatory flow with a parabolic velocity profile.

Scaled relative to the water depth h and to the friction velocity u_*, the vertical jumps are chosen by Allen (1982) to have length and velocity scales

$$L' = 0{\cdot}1, \quad w' = 1{\cdot}0975. \tag{7.1}$$

This choice was motivated by the experimental results of Sullivan (1974). Thus the effective (long-term) vertical diffusivity is given by

$$\kappa = \tfrac{1}{2}L'w' = 0{\cdot}055 \tag{7.2}$$

(Csanady 1973, equation (2.30)). Also, the dimensionless tidal period and horizontal tidal velocity are chosen (as per the Mersey Narrows):

$$T = 89{\cdot}4, \quad U' = 19{\cdot}8 \quad (U = 5{\cdot}6). \tag{7.3}$$

We remark that with these parameters (7.2), (7.3) the dimensionless frequency Ω has the small value

$$\Omega = 0{\cdot}13, \tag{7.4}$$

with the consequences that the dispersion process is quasi-steady and the contraction of the contaminant cloud will be imperceptible (Allen 1982, figure 8).

Figures 4 (a, b, c) compare the random-walk and Gaussian concentration distributions at the levels $z/h = -0{\cdot}05$, $-0{\cdot}55$, $-0{\cdot}95$ when $\omega t = \frac{1}{2}\pi$, $\omega t_0 = 0$. The fluctuations in the random-walk results could have been reduced if either the horizontal resolution had been coarser, or more than 10^4 particles had been used. Despite the relatively rapid vertical mixing, there is a noticeable shift between the concentration distributions near the free surface and near the channel bed. This is likewise evident in the Gaussian approximation. Indeed, there is reasonable agreement between the two approaches.

Figure 5 gives the corresponding comparison for the vertically averaged concentration $\bar{c}$. The vertical averaging reduces the fluctuations. However, it also gives rise to skewness ($-0{\cdot}16$) and kurtosis ($-0{\cdot}50$). These features could not be reproduced with a diffusion model for $\bar{c}(x,t)$. However, the two-dimensional Gaussian approximation yields suitably non-Gaussian results for $\bar{c}$.

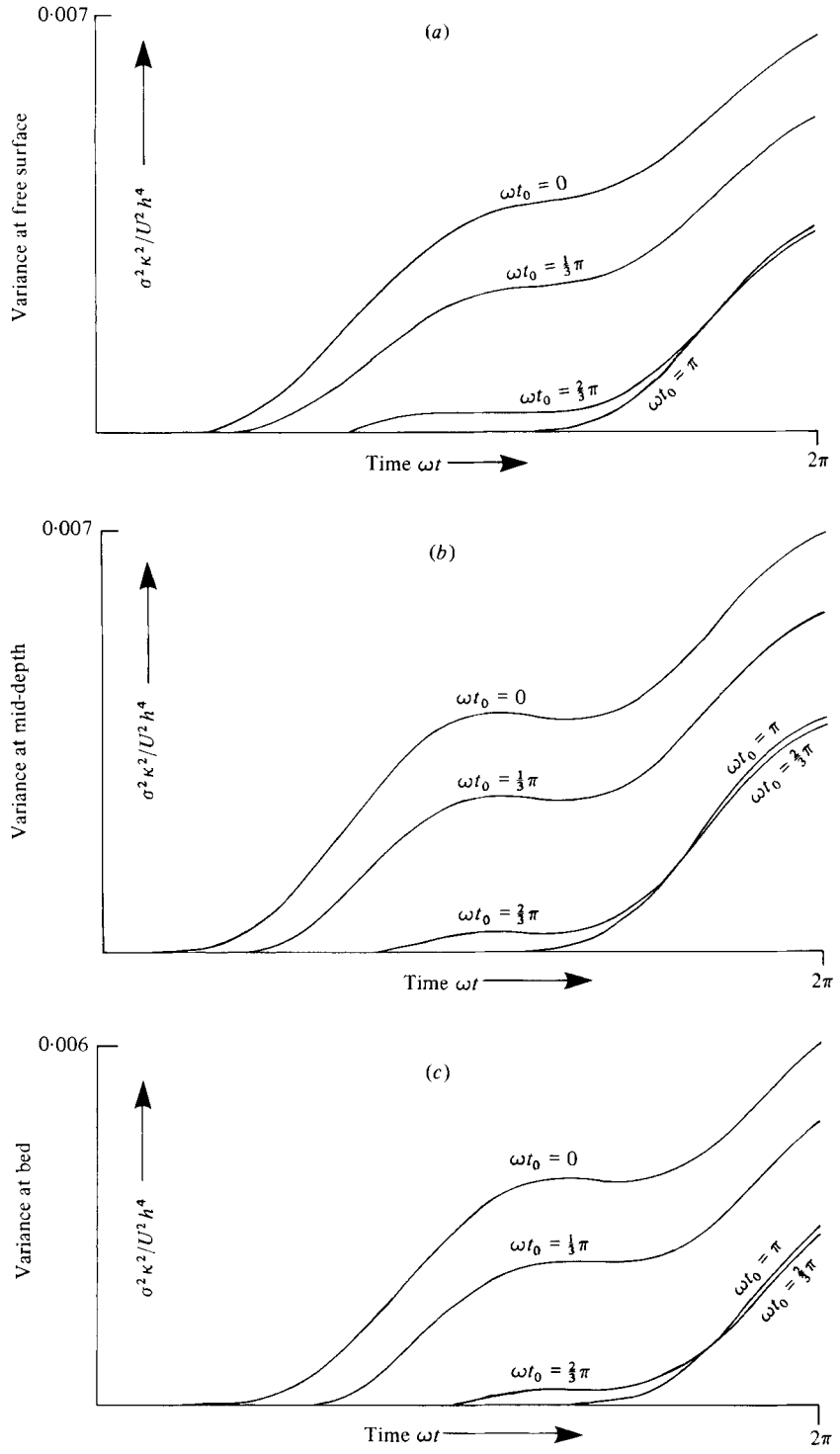

FIGURE 3. Variances as a function of time at the depths (*a*) $z = 0$, (*b*) $z = -\frac{1}{2}h$, (*c*) $z = -h$ in an oscillatory flow with a parabolic velocity profile.

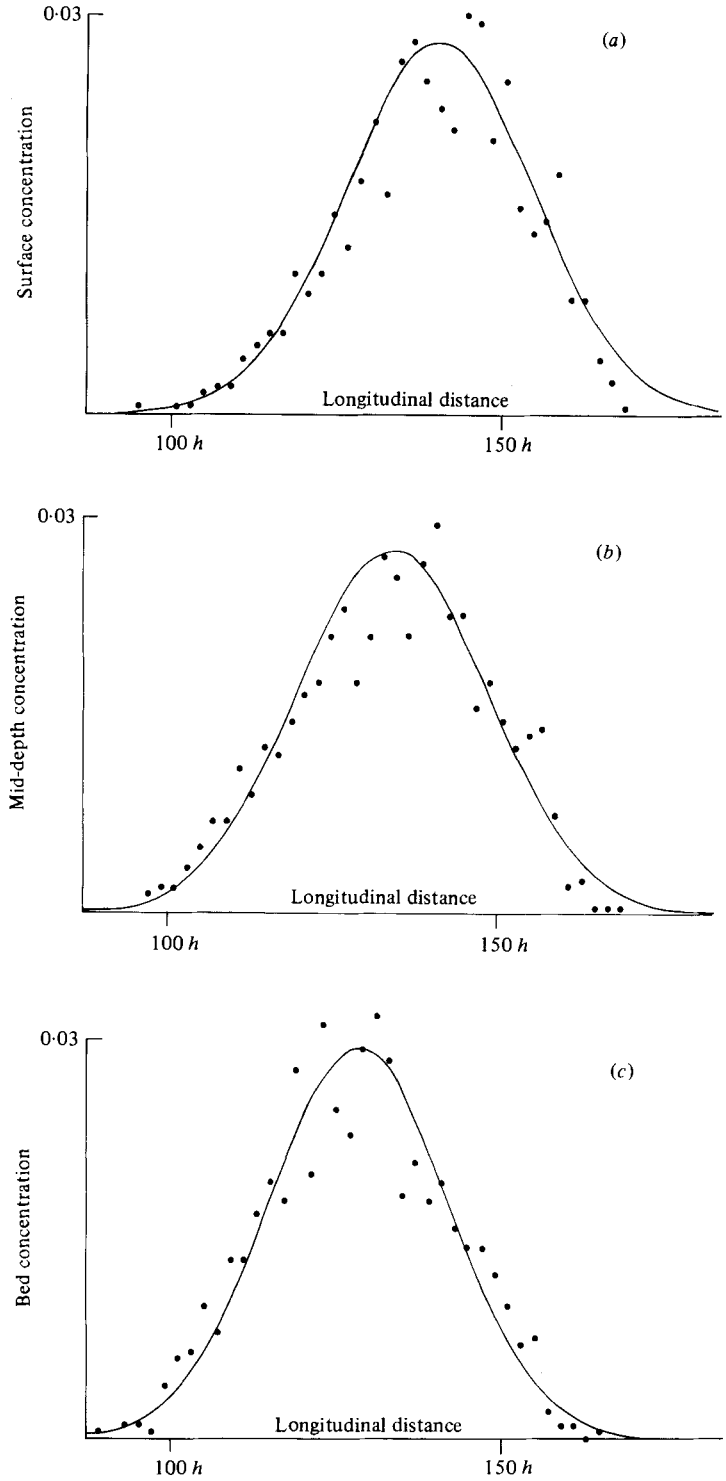

FIGURE 4. Comparison between Allen's random-walk results and the Gaussian approximation a quarter-cycle after discharge at the levels (*a*) $z = -0{\cdot}05h$, (*b*) $z = -0{\cdot}55h$, (*c*) $z = -0{\cdot}95h$.

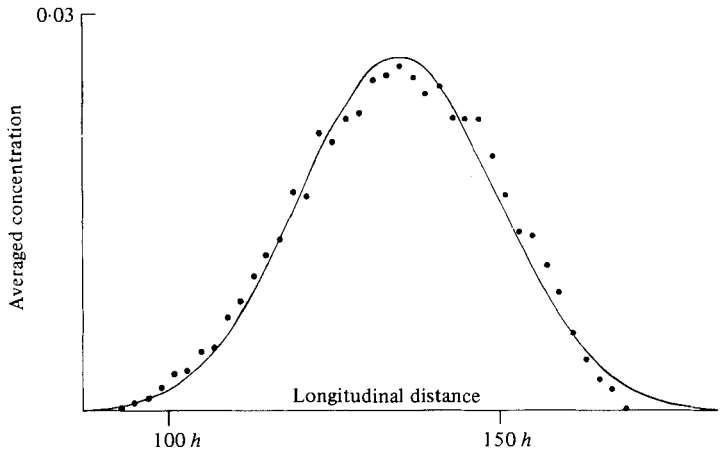

FIGURE 5. Comparison between Allen's random-walk results and the Gaussian approximation at a quarter-cycle after discharge for the vertically averaged concentration.

8. A simple model for lateral shear dispersion in a shallow estuary

The complexity of the results (3.8), (4.7), (4.11), (4.12) for X and V stems from the occurrence of infinite series. Thus a recipe for a simple model would be to truncate the series. This arises naturally if the velocity profile $u(y, z, t)$ were to involve just a single mode:

$$u(y,z,t) = \bar{u}(t) + u_2(t)\,\psi_2(y,z). \tag{8.1}$$

In shallow estuaries (less than 20 m deep), the timescale for vertical mixing is very much less than the tidal period. Thus on a tidal timescale we can ignore vertical concentration variations, and the vertically integrated eigenmode equation (3.1a) becomes

$$\frac{d}{dy}\left(h\langle\|\kappa\|\rangle\frac{d\psi_m}{dy}\right) + \lambda_m h\psi_m = 0, \tag{8.2a}$$

with

$$h\langle\|\kappa\|\rangle\frac{d\psi_m}{dy} = 0 \quad \text{at} \quad y = y_-, y_+. \tag{8.2b}$$

Here $h(y)$ is the water depth, $\|\kappa\|$ the vertically averaged transverse diffusivity, and y_-, y_+ are the two sides of the estuary.

A reasonable model for the velocity and diffusivity distributions across the estuary is

$$\|u\| = \frac{\bar{u}h\bar{h}}{\bar{h}^2}, \quad \|\kappa\| = 0{\cdot}02\,|\bar{u}|\,h \tag{8.3a, b}$$

(Fischer 1972). For a parabolic depth profile

$$h(y) = H\left[1 - \left(\frac{y}{B}\right)^2\right], \tag{8.4}$$

the eigenmodes are ultraspherical polynomials

$$\psi_m = \left[\frac{2(2m+3)}{3(m+1)(m+2)}\right]^{\frac{1}{2}} C_m^{(\frac{3}{2})}\left(\frac{y}{B}\right), \tag{8.5a}$$

$$\lambda_m = m(m+3)\,0{\cdot}02\,\frac{\langle|\bar{u}|\rangle H}{B^2} \tag{8.5b}$$

(Abramowitz & Stegun 1965, §22). Conveniently, the velocity profile involves just the $m = 2$ mode (Smith 1982*a*, §6):

$$\|u\| = \bar{u} - (\tfrac{1}{14})^{\frac{1}{2}} \bar{u} \psi_2\left(\frac{y}{B}\right) \tag{8.6a}$$

$$= \bar{u} - \tfrac{1}{4}\bar{u}\left[5\left(\frac{y}{B}\right)^2 - 1\right]. \tag{8.6b}$$

Such is the extent of the mathematical simplifications that it is not necessary to employ the full analysis of §§3, 4. Instead, we can solve the high-Péclet-number version of (3.3*a*), (4.1*a*) directly to obtain

$$X = \frac{1}{4}\left[1 - 5\left(\frac{y}{B}\right)^2\right] F(t, t_0), \tag{8.7a}$$

with

$$F(t, t_0) = \int_{t_0}^{t} \bar{u}(t') \exp\left(-\lambda_2 T(t', t)\right) dt', \tag{8.7b}$$

$$\sigma^2 = \frac{1}{4}\int_{t_0}^{t} \frac{\|\kappa(t')\|}{\langle\|\kappa\|\rangle} F(t', t_0)^2 \lambda_2 \, dt' - \frac{1}{4}\left[1 - 5\left(\frac{y}{B}\right)^2\right] \int_{t_0}^{t} \exp\left(-\lambda_2 T(t', t)\right) \frac{\|\kappa(t')\|}{\langle\|\kappa\|\rangle} F(t', t_0)^2 \lambda_2 \, dt'. \tag{8.8}$$

(In this context the high-Péclet-number approximation is equivalent to the estuary width squared greatly exceeding the depth squared.) From the y-dependent term in (8.8) we can verify that, as the centroid displacement factor F passes through zero, the variance is decreasing at the two sides of the flow:

$$\sqrt{\tfrac{1}{5}} < \left|\frac{y}{B}\right|. \tag{8.9}$$

As an illustrative example, figures 6 and 7 show the evolution of X and σ^2 for the particular case

$$H = 10 \text{ m}, \quad B = 200 \text{ m}, \quad \omega = 1{\cdot}5 \times 10^{-4} \text{ s}^{-1},$$
$$\|\kappa\| = 0.02h\|u\|, \quad \bar{u} = \sin \omega t \text{ (m s}^{-1}\text{)}, \tag{8.10}$$

and for the discharges at the turn of the tide $\omega t_0 = 0$, and at the flood $\omega t_0 = \frac{1}{2}\pi$. For this moderately wide estuary the oscillatory character and y-dependence of the variance is quite marked for several tidal cycles. Also, via the F^2 factors, there is a strong dependence of the rate of spreading upon the precise time of discharge.

This dramatic memory effect has been investigated recently by the author (Smith 1982*b*) in the context of discharges in the deep ocean. If the uniform contaminant release takes place at the extreme of the particle displacement $\omega t_0 = 0$, then the deformation of the concentration contours (and hence the concentration gradient across the flow) is maximized. Thus the shear-dispersion mechanism is at its most efficient, with a correspondingly rapid rate of spreading of the contaminant. If instead the contaminant release takes place at mid-cycle $\omega t_0 = \frac{1}{2}\pi$, then the deformation of the concentration contours is symmetrical and is minimized (in a least-square sense). This means that for the first few cycles the shear-dispersion mechanism is at its least efficient. Eventually (on a timescale of $1/\lambda_2$) the memory of the precise discharge time fades away. However, there is a persistent y-independent shift in σ^2 (the excess variance). In wider estuaries this effect is more pronounced and the timing of a discharge is even more critical.

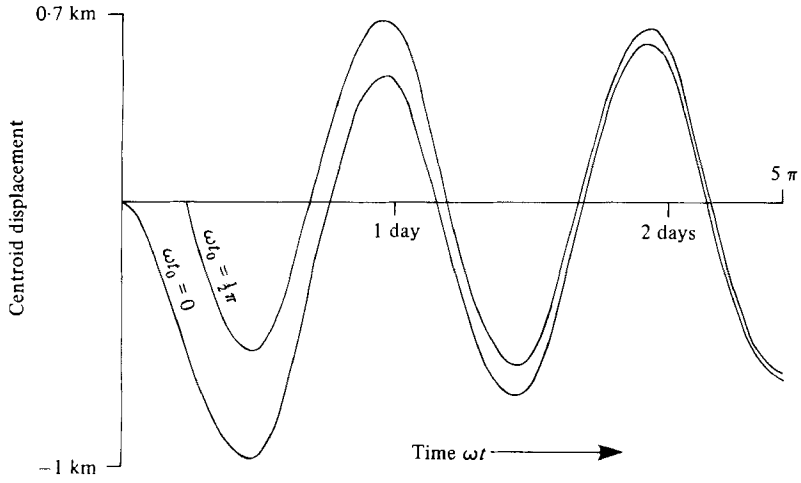

FIGURE 6. Centroid displacement as a function of time at the position $y = B$ in a shallow estuary with a parabolic depth profile.

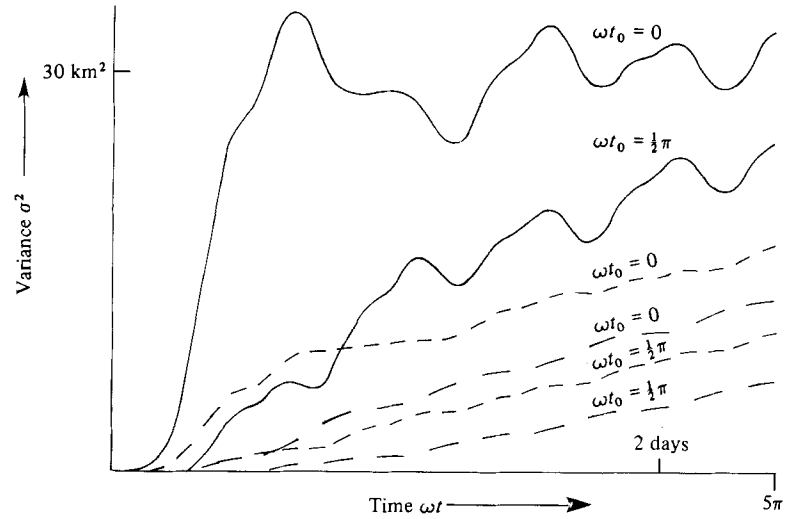

FIGURE 7. Variance at the side (——), centre (— — —), and at $y/B = \sqrt{\frac{1}{5}}$ (— —) for discharges at the turn of the tide and at the flood in a shallow estuary with a parabolic depth profile.

I wish to thank Dr Catherine Allen for allowing me to use her random-walk results. The financial support of British Petroleum and the Royal Society is gratefully acknowledged.

REFERENCES

ABRAMOWITZ, M. & STEGUN, I. A. 1965 *Handbook of Mathematical Functions*. Dover.

ALLEN, C. M. 1982 Numerical simulation of contaminant dispersion in estuary flows. *Proc. R. Soc. Lond.* **A381**, 179–184.

ARIS, R. 1956 On the dispersion of a solute in a fluid flowing through a tube. *Proc. R. Soc. Lond.* **A235**, 67–77.

BOWDEN, K. F. 1965 Horizontal mixing in the sea due to a shearing current. *J. Fluid Mech.* **21**, 83–95.

BOWDEN, K. F. & FAIRBAIRN, L. A. 1952 A determination of the frictional forces in a tidal current. *Proc. R. Soc. Lond.* **A214**, 371–392.

CHATWIN, P. C. 1970 The approach to normality of the concentration distribution of a solute in a solvent flowing along a straight pipe. *J. Fluid Mech.* **43**, 321–352.

CHATWIN, P. C. 1975 On the longitudinal dispersion of passive contaminant in oscillatory flows in tubes. *J. Fluid Mech.* **71**, 513–527.

CSANADY, G. T. 1973 *Turbulent Diffusion in the Environment.* Reidel.

FISCHER, H. B. 1972 Mass transport mechanisms in partially stratified estuaries. *J. Fluid Mech.* **53**, 671–687.

HOLLEY, E. R., HARLEMAN, D. R. F. & FISCHER, H. B. 1970 Dispersion in homogeneous estuary flow. *J. Hydraul. Div. A.S.C.E.* **96**, 703–724.

SMITH, R. 1982*a* Contaminant dispersion in oscillatory flows. *J. Fluid Mech.* **114**, 379–398.

SMITH, R. 1982*b* Dispersion of tracers in the deep ocean. *J. Fluid Mech.* **123**, 131–142.

SMITH, R. 1982*c* Gaussian approximation for contaminant dispersion. *Q. J. Mech. Appl. Math.* **35**, 345–366.

SULLIVAN, P. J. 1974 Instantaneous velocity and length scales in a turbulent shear flow. *Adv. Geophys.* **18A**, 213–223.